Proc. Natl. Acad. Sci. USA
Vol. 94, pp. 14826–14831, December 1997
Neurobiology

Vascular imprints of neuronal activity: Relationships between the dynamics of cortical blood flow, oxygenation, and volume changes following sensory stimulation

(hemodynamics/blood oxygenation/laser Doppler flowmetry/cerebral microcirculation/optical imaging)

DOV MALONEK*†, ULRICH DIRNAGL‡, UTE LINDAUER‡, KATSUYA YAMADA§, IWAO KANNO¶, AND AMIRAM GRINVALD*

*Department of Neurobiology, Weizmann Institute of Science, Rehovot 76100, Israel; ‡Experimental Neurology, Department of Neurology, Charité Hospital, Humboldt University, Berlin, Germany; §Department of Physiology, Akita University School of Medicine, Akita, 010 Japan; and ¶Department of Radiology and Nuclear Medicine, Akita Research Institute of Brain and Blood Vessels, Akita, 010 Japan

Communicated by Louis Sokoloff, National Institutes of Health, Bethesda, MD, October 24, 1997 (received for review June 9, 1997)

ABSTRACT **Modern functional neuroimaging methods, such as positron-emission tomography (PET), optical imaging of intrinsic signals, and functional MRI (fMRI) utilize activity-dependent hemodynamic changes to obtain indirect maps of the evoked electrical activity in the brain. Whereas PET and flow-sensitive MRI map cerebral blood flow (CBF) changes, optical imaging and blood oxygenation level-dependent MRI map areas with changes in the concentration of deoxygenated hemoglobin (HbR). However, the relationship between CBF and HbR during functional activation has never been tested experimentally. Therefore, we investigated this relationship by using imaging spectroscopy and laser-Doppler flowmetry techniques, simultaneously, in the visual cortex of anesthetized cats during sensory stimulation. We found that the earliest microcirculatory change was indeed an increase in HbR, whereas the CBF increase lagged by more than a second after the increase in HbR. The increased HbR was accompanied by a simultaneous increase in total hemoglobin concentration (Hbt), presumably reflecting an early blood volume increase. We found that the CBF changes lagged after Hbt changes by 1 to 2 sec throughout the response. These results support the notion of active neurovascular regulation of blood volume in the capillary bed and the existence of a delayed, passive process of capillary filling.**

There is a tight coupling between electrical activity in the brain and both cellular metabolism and hemodynamic changes, as shown in the pioneering work of Roy and Sherrington (1), Ketty and Schmidt (2), Sokoloff *et al.* (3), and Chance *et al.* (4). This coupling is used by modern, functional neuroimaging methods, like positron-emission tomography (PET) (5, 6), optical imaging (7, 8), and functional MRI (fMRI) (9–11) to obtain, indirectly, maps of neuronal activity. These imaging techniques rely on various types of activity-dependent changes: regional changes in cerebral blood flow (CBF) were first used for functional mapping of the brain by PET studies and subsequently by single photon emission computed tomography (SPECT) and by flow-sensitive MRI. The optical imaging technique relies on color changes associated with either cerebral blood oxygenation changes or blood volume changes (CBV) and produces maps of the functional architecture of the cortex at a spatial resolution even higher than that needed to resolve individual functional domains (7, 8). These high-resolution optical maps provide evidence for a very precise spatial match between cortical electrical activity and localized changes in blood deoxyhemoglobin concentration (HbR). HbR and CBV changes are also used for human brain mapping in blood oxygenation level-dependent (BOLD) fMRI, a technique that was developed soon after optical imaging (10–12).

Although CBF, CBV, and HbR changes have been used to obtain functional maps of neuronal electrical activity, little is known about the dynamics of neurovascular coupling, the underlying mechanisms, and the cortical metabolic processes affecting these changes. Controversies have emerged because of difficulties in interpreting the signals measured by the above imaging techniques, in characterizing and quantifying the metabolic processes, and in selectively measuring hemodynamic changes (e.g., HbR without CBV) from each vascular compartment.

By using imaging spectroscopy, which allows selective measurement of both HbR and HbO_2, we have recently demonstrated (13) that Hb-oxygenation changes in response to neuronal activation are biphasic; an early (<3 s), localized increase in HbR (often referred to as the "initial dip") is followed by a delayed decrease in HbR and a concomitant increase in HbO_2. Furthermore, the HBO_2 increase is spatially less well registered with the activated cortical columns relative to the early HbR increase [figure 3 in Malonek and Grinvald (13)]. A possible implication of these findings is that the early deoxygenation may provide a higher spatial resolution for fMRI neuroimaging than the conventionally used delayed hyperoxygenation response. Furthermore, the early Hb-deoxygenation-based methods may provide higher spatial resolution than CBF-based methods.

The time course of the HbR change and the existence of the "initial dip" has been confirmed only recently by high magnetic field fMRI (14), raising the question of what, precisely, is being measured by most other BOLD fMRI studies. It is therefore necessary to clarify the temporal relationship between cerebral blood flow, volume, and oxygenation during functional activation. This has never been determined experimentally. In this study we therefore investigate this relationship and specifically address the following questions. Is the early activation-induced increase in HbR caused by an increase in cerebral metabolic rate of oxygenation ($CMRO_2$) without matching CBF response? Does an increase in resting CBF affect the activation-induced changes? The answers to these questions are not only relevant to functional neuroimaging in humans, but may also further our understanding of the basic mechanisms of neurovascular coupling.

The publication costs of this article were defrayed in part by page charge payment. This article must therefore be hereby marked "*advertisement*" in accordance with 18 U.S.C. §1734 solely to indicate this fact.

Abbreviations: PET, positron-emission tomography; fMRI, functional MRI; CBF, cerebral blood flow; CBV, cerebral blood volume; BOLD, blood oxygenation level dependent; LDF, laser Doppler flowmetry.

†To whom reprint requests should be addressed.

MATERIALS AND METHODS

This study is based on experiments performed in six cats. In two of the cats conventional optical imaging of intrinsic signals was performed in combination with laser Doppler flowmetry (LDF). In the other four cats, imaging spectroscopy (optical imaging with high spectral resolution) was performed concurrently with the LDF. The procedures for conventional optical imaging, imaging spectroscopy, and LDF are outlined below in chronological order during a typical experiment. Additional details may be found in previous publications for optical imaging (7, 8, 15), imaging spectroscopy (13), and LDF (16–18).

Animals. Anesthesia was induced by ketamine hydrochloride (10–20 mg/kg i.m.) followed by sodium pentothal (20 mg/kg per h, i.v.). A headset was implanted over the anterior part of the skull to allow attachment of the head with minimal trauma. Animals were then placed in the stereotactic apparatus by using the headset attachment. A round opening was cut in the skull overlying area 17 and 18 and the dura was carefully resected. A cranial window chamber filled with inert solution and sealed with a transparent disk was placed over the opening and anchored to the skull with screws and dental cement. The animals were paralyzed (succinylcholine hydrochloride, 20 mg/kg/h) and artificially respirated. They received anesthetics and paralytics throughout the experiment and the heart rate, EEG, end-tidal CO_2, and temperature were constantly monitored. Blood pressure was monitored during the last four experiments. The corneas were fitted with zero power contact lenses and atropine (1%) was administered to paralyze accommodation. The eyes were focused on a tangent screen at a distance of 57 cm by using appropriate lenses, as determined by retinoscopy.

Visual Stimulation. The primary stimuli that were used in this study were vertical and horizontal moving gratings (high contrast, 0.3 cycles/degree; duty cycle = 0.2, 18°/sec) and a blank screen. The stimulation was binocular all along, with both eyes converged and focused on a stimulus screen [distance = 57 cm, extent = 40° (h) × 30°(v) contralateral to the imaged hemisphere]. During each experiment, the different stimuli were presented for 2–10 sec followed by a blank screen for an additional 15–30 sec. Each stimulus was presented 24–64 times during each experiment, and the order of appearance was randomized. Each curve in the figures is the calculated average of these repetitions.

Optical Imaging. Procedures were similar to those described elsewhere (7, 8, 15). In brief, intrinsic optical signals evoked by the visual stimuli were recorded by using an enhanced video system (Imager 2001, Optical Imaging, Germantown, MD) attached to a macroscope (19). The exposed cortex was illuminated with orange or green light (570 or 605 nm), and the reflected light was collected by the camera through the glass window of the chamber. Images were acquired at 2 Hz and stored to disk.

Imaging Spectroscopy. Procedures were similar to those described in an earlier publication (ref. 13; for *in vivo* single location spectral measurements, see ref. 20). In brief, the cortex was examined by using a two-tandem-lens macroscope that formed two image planes. The image in the first image plane was masked by an opaque disk with a transparent slit that was positioned in a selected image location, which showed a marked segregation of orientation columns. A dispersing grating, whose grooves were parallel to that slit, was positioned between the objective and the imaging lens of the second macroscope. Thus, the recorded image (second image plane) represented multiple displaced images of the slit, the degree of displacement varying with wavelength. We refer to these images as spatiospectral images. The spatial resolution of our spectroscope was better than 200 μm in the relevant spectral range, and the spectral resolution was better than 4 nm.

Laser Doppler Flowmetry. A main goal of this study was to temporally and spatially correlate activity-dependent Hb-oxygenation changes with changes in regional cerebral blood flow (rCBF).

LDF (21) is based on the recording of the Doppler shifts that occur when mobile red blood cells scatter monochromatic light. Principles and technical details have been described elsewhere in great detail (22, 23). A number of studies have validated the use of LDF to measure quantitatively changes in rCBF (16–18). However, absolute CBF values (blood perfusion per tissue volume) measured with LDF do not correlate well with quantitative CBF as measured with [^{14}C]iodoantipyrine autoradiography and hence were not used in this study. The sample volume of LDF is affected mainly by probe geometry, wavelength, and distance of the probe from the tissue. With the equipment and setup used here, the sample volume was estimated to be approximately 1 mm^3.

We used a Periflux 4001 (Perimed, Stockholm; wavelength of 780 nm) laser Doppler flowmeter to which a needle probe (Perimed PF 403; outer diameter, 450 μm; fiber separation, 250 μm) was attached. The probe was advanced at an angle of 45° through a tightly sealed hole in the cover glass of the cranial window and reached a position <1 mm from the brain surface. By using the imaging spectroscope, the positioning of the probe and thus the focus of the sample volume were checked and adjusted by visual monitoring of the near-infrared spot projected on the brain surface by the laser beam (Fig. 1*A*). Thus, a complete spatial registration of cortical area monitored by imaging spectroscopy and LDF was attained. The time constant of the LDF was set to 0.03 seconds, and the LDF readings were digitized at 100 Hz, transferred to computer memory, and saved to disk. We also verified that the delay of the LDF response to an instantaneous flow change was shorter than 0.1 sec.

Experimental Procedure. The experiment was carried out as follows. First, optical imaging of orientation maps was performed through the double-tandem-lens system. Images of the exposed cortical surface (epi-illumination with 100-W halogen lamp, λ = 605 nm) were collected, and functional orientation maps were obtained by computing the difference between images obtained during visual stimulation by moving gratings of orthogonal orientations. Only after observing segregated orientation columns in the calculated differential functional maps did we continue with the spectroscopic and LDF measurements. The optical imaging system was modified into an imaging spectroscope, and a broad-spectrum light source (500–700 nm) was used to illuminate the cortical surface [details in Malonek and Grinvald (13)]. The data collection procedure remained unchanged: spatiospectral images were accumulated by the video camera and digitized at a video rate of 25 Hz. These frames were averaged on-line, lowering the time resolution to 2 Hz for the off-line analysis. The LDF probe was inserted through the rubber gasket and targeted to the same cortical area.

Data acquisition of the LDF, optical imaging, and imaging spectroscopy were synchronized to the respirator and heart beat as described elsewhere (7, 8, 15).

Spectral Analysis. From the intensity variations in the image it was possible to obtain the reflection spectrum of each image point along the slit. The intensity profile of a given horizontal line represented the reflection spectrum of a given location in the imaged specimen. Horizontal lines at right angles to these had an intensity profile that represented the variation along the selected slit-like image of cortex at a given wavelength. The comparison of reflection spectra taken from different locations was readily performed by comparing the intensity profiles from the appropriate locations within a single image. The spatiospectral images were analyzed by comparing the images acquired during visual stimulation with those acquired during

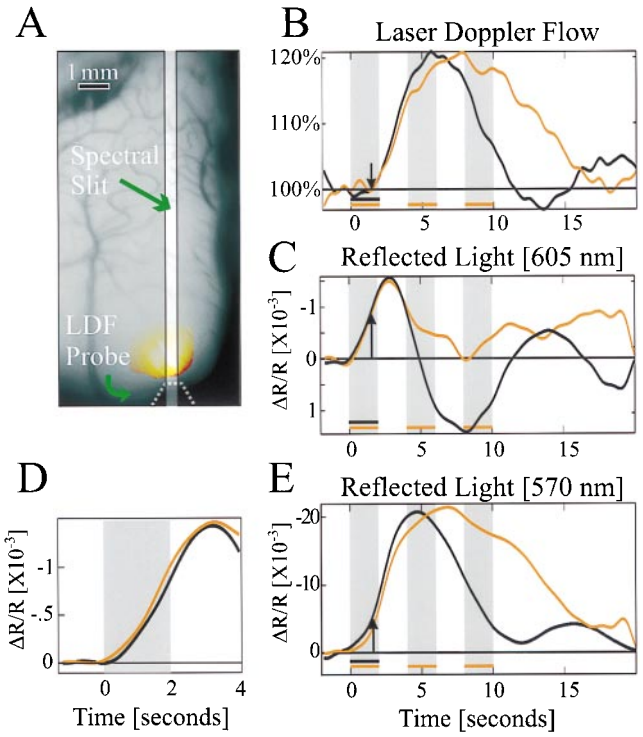

FIG. 1. Simultaneous measurement of cortical reflection and CBF. (*A*) An image of the cortical surface, the location of slit used for imaging spectroscopy, the tip of LDF probe, and the reflection of its beam from the cortex. The yellow spot marks the cortical region that was illuminated by the LDFs laser during the measurements. (*B*, *C*, and *E*) Cortical response to visual stimulation. Black curves represent response to short stimulus (2 sec), and red curves represent its response to long stimulus (10 sec, composed of 2 on, 2 off, 2 on, 2 off, 2 on). Each curve is the average response to 24 stimulation periods during a single experiment. (*B*) LDF response. Its onset (arrow) lags after stimulus onset by ≈1.5 sec. (*C*) Cortical reflection change: 605-nm illumination. The response is biphasic, and its onset leads the LDF response by ≈1 sec. Long stimulus duration attenuates the second phase, which almost vanishes. Notice that increased reflection is downward. (*D*) The vascular response ("initial dip") at different flow levels and at different times after the stimulus onset. We compare the early response to the short stimulus (black curve in *C*), when CBF was at equilibrium, with that obtained when CBF was elevated and a second delayed stimulus followed, by subtracting the short stimulus curve from the long stimulus curve (red curve in *C*). In *D*, when this difference, i.e., the net response to the second stimulus, shown in red, is shifted in time and superimposed on the response to the first stimulus (black line), the two curves are nearly identical. The second stimulus was given when CBF increased by ≈15%. (*E*) Cortical reflection change: 570-nm illumination. Similar to reflection changes at 605-nm illumination, the response onset leads the LDF response by 1 sec. The response is maintained throughout stimulus duration, for both short and long durations.

blank screen. Changes in the reflected light were modeled by the following formula:

$$\Delta R_\lambda(t) = K_1(t)\cdot\varepsilon_{HbO_2} + K_2(t)\cdot\varepsilon_{HbR} + LS(t) + E(t),$$

where $K_1(t)$ is a relative parameter related to the product of HbO_2 and the optical pathlength, and $K_2(t)$ is similarly related to HbR. $LS(t)$ (light scattering) is related to changes of the tissue's refractive index, and $E(t)$ is the residual error term. By using a linear least squares fit routine, the above equation was fit to the intensity profile along each line in each spatiospectral image, for a spectral range of 530–650 nm. The fit was good and the root mean square of error (difference between the measurements and the modeled curve) was less than 5% in most experiments. Other models for the light-scattering contribution neither improved the goodness of fit nor changed the main results outlined here for HbR and HbO_2.

RESULTS

Stimulus-Evoked CBF and Optical Reflectance Responses. To compare CBF changes to optical reflectance changes we simultaneously measured the time course of the CBF and the activity-dependent reflected signals at either one of two wavelengths (605 and 570 nm) in response to visual stimulation. A short, 2-sec visual stimulation with moving-oriented gratings induced both blood flow (Fig. 1*B*) and reflectance changes (Fig. 1 *C* and *E*), which persisted for more than 10 sec (black curves). The cortical reflectance changes at 605 ± 5 nm illumination (Fig. 1*C*) had a stereotypical biphasic shape; an initial decrease in reflectance ($\Delta R/R = -1.5 \times 10^{-3}$) followed by an increase in cortical reflectance ($\Delta R/R = 1.5 \times 10^{-3}$; a decreased reflectance, i.e., cortical darkening, is assigned negative numbers but plotted upward). The observed reflectance changes result from changes in both light absorption and light scattering in the tissue. The dynamics of CBF changes were strikingly different (Fig. 1*B*): the onset (arrows in Fig. 1 *B*, *C*, and *E*) was delayed by more than 1 sec after the reflectance signal onset, and its shape was monophasic rather than biphasic. The CBF response reached its maximal change of ≈20% approximately 4 sec after stimulus termination and returned to baseline within an additional 8 sec. The dynamics of CBF changes observed here (Fig. 1*B*) were in good agreement with previous LDF studies (24).

It already has been shown that changes in cortical reflectance at 605 nm can be used to approximate HbR changes, whereas at 570 nm (Hb-isosbestic point), blood volume changes are emphasized (7, 13). As in previous observations, cortical reflection changes at 570 nm (Fig. 1*E*) were markedly different from those at 605 nm (Fig. 1*C*). However, the blood volume changes (major component of curve in Fig. 1*E*) and the CBF-LDF curves (Fig. 1*B*) display an apparent similarity, indicating that flow and volume dynamics are more similar than flow and HbR changes. The major exception is at short latencies, where, as at 605 nm, the onset of the reflected light response at 570 nm precedes the onset of the blood flow response (indicated by the arrow) by more than a second. This suggests that the blood flow onset is delayed relative to the onset of both HbR and blood volume increases.

To study the responses to longer stimulation we used a train of three short stimuli (interlaced periods of 2 sec of grating stimulus, 2 sec of blank stimulus). CBF and cortical reflection (605-nm illumination) were altered differently, whereas CBF continued to increase and remained elevated throughout the stimulation; by contrast, the second phase of cortical reflectance at 605 nm was reduced (Fig. 1 *B* and *C*, red curves). Again, the blood volume change estimated by the 570-nm measurement was similar to the CBF response, except in the period immediately after the onsets of both responses.

Dynamics of Stimulus-Evoked CBF, Blood Oxygenation, and Total Hemoglobin Responses. Reflectance measurements at a single wavelength, as the ones described above, cannot be used to estimate HBO_2 and are only a first approximation for HbR and blood volume changes. To quantify various biochemical and physiological manifestations of the cortical response to activation we employed imaging spectroscopy. By using this technique, we measured cortical reflectance changes at multiple wavelengths and multiple locations simultaneously as a function of time. From these spectra we extracted the time course of the changes in the individual components, HbR, HBO_2, and Hbt (see *Methods*) and compared them with the simultaneously measured CBF response (Fig. 2). We found a striking similarity between the HbO_2 and CBF responses (Fig. 2); the CBF and HBO_2 curves are almost identical in their

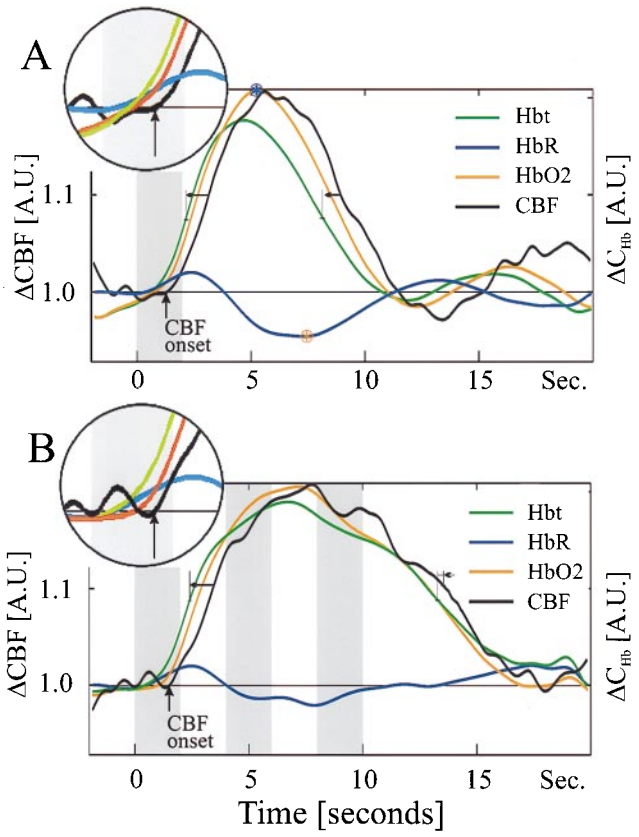

FIG. 2. Dynamics of various vascular responses. Total hemoglobin concentration (Hbt, green line) leads CBF response (black line) throughout the response cycle for both the short stimulus (*A*) and the repeated stimuli (*B*). Each curve is the average response to 24 stimulation periods during a single experiment. Horizontal arrows mark the temporal difference between the curves when they had reached 50% of their maximal amplitude (marked by thin, vertical lines) during the uprising phase and during the decay to baseline. HbR curve appears to lead all other components, and it reaches its peak before all other curves. Notice the delays of both the CBF (marked by arrow) and the HbO_2 onsets after the stimulus onsets. At onset, Hbt change is entirely composed of HbR elevation, whereas at the later phase it is predominantly HbO_2. Because of fluctuations of HbO_2 (and thus Hbt) before stimulation, its onset is determined as time when its rate of change increased. Asterisks mark the maximum of HbO_2 and the minimum of HbR.

onset, rise time, and decay to baseline for both short- and long-stimulus durations.

The dynamics of the HbR response was drastically different from both CBF and HbO_2 responses (Fig. 2). Its time course (blue curve) had a stereotypical biphasic shape as compared with the monophasic shapes of both the CBF and the HbO_2 curves. Furthermore, the onset of the HbR increase preceded the onset of CBF increase by more than a second (e.g., Fig. 2*B Inset*) whereas its time to peak was shorter by more than 3 sec. The delayed onset of CBF response (>1.3 sec) was observed repeatedly in all the experiments during this study ($n = 6$). This is consistent with the interpretation that the HbR time course results from two competing mechanisms; the early HbR increase is a result of an increase in $CMRO_2$, whereas the later increase in CBF causes the reduction in HbR and the subsequent undershoot. Note that the time course of HbR (Fig. 2) resembles that of the cortical reflection change at 605 nm (Fig. 1*C*, black), which has been used as an approximation for this chromophore.

To shed light on the mechanisms that underlie these events in microcirculation, we focused on the first 2 sec of the response (Fig. 2 *Insets*). During the initial first second of functional activation, the only observable change was indeed an increase in deoxyhemoglobin (i.e., increase in HbR), and no change in CBF was observed during this phase (Fig. 2). At 1 sec after stimulation, the elevated HbR has reached ≈30% of its peak value whereas the change in CBF (if at all occurred) was less than 4% of its peak value (Figs. 1*B* and 2*A Inset*). These observations, together with the lack of a concomitant decrease in HbO_2, imply that during this period an increase in total hemoglobin concentration ($\Delta Hbt = \Delta HbR + \Delta HbO_2$) occurred (Fig. 2, green lines). Thus, we suggest that the activity-induced rise in $CMRO_2$ leads to an increased extraction of O_2 and a simultaneous but independent increase in the total hemoglobin concentration. This is at a time when CBF has not yet started to increase in response to the stimulus. Further examination of the different curves showed that the rate of change in HbR started to decrease at the onset of both CBF and HbO_2 changes (see also Fig. 3). One likely interpretation is that arteriolar vasodilatation causes an outwash of the increased HbR produced by the increased oxygen consumption ($CMRO_2$). During the phase of increased cerebral blood flow leading to blood hyperoxygenation, HbR is no longer a measure of the increased oxygen consumption exclusively, but rather reflects the net effect of $CMRO_2$-induced blood deoxygenation together with the flow-induced blood hyperoxygenation.

We further observed that the stimuli with short duration elicited concentration changes that continued for a long time after their termination. HbO_2, Hbt, and CBF continued to increase and reached a maximum only after 5 sec, and at the same time HbR decreased (Fig. 2*A*). A delay between the time point at which CBF reached its maximum and the time point when HbR reached its minimum was observed (asterisks in Fig. 2*A*). This is in contrast with the inverse relationship observed after the onset of stimulation, when HbR leads the CBF response by more than a second. This delay is compatible with the assumption that $CMRO_2$ starts to diminish before CBF starts to decline.

The temporal relations between Hbt and CBF can shed light on the underlying vascular regulatory processes (Fig. 2). The changes in Hbt lead the changes in CBF by more than a second throughout the response. The initial increase in Hbt was composed primarily of an increase in HbR, and thus early in the response, HbR changes lead the changes in CBF. At a later phase, Hbt changes were composed primarily of HbO_2 changes, which lead the changes in CBF and HbR.

To emphasize the temporal relationships of CBF, HbR, and Hbt we display the same results in the form of phase plots: ΔHbR vs. ΔCBF (Fig. 3*A*) and ΔHbt vs. ΔCBF (Fig. 3*B*). In these plots, a simultaneous covariation of the parameters appears as a straight, tilted line, whereas a delayed covariation appears as a curved line or a tilted ellipsoid.

After the initial increase of HbR and the delayed onset of a CBF change (arrow in Fig. 3*A*), the phase plot transforms into a curved line, indicating the inverse but delayed variation of both ΔHbR and ΔCBF. At the final phase of the response (its onset marked by an asterisk), these parameters co-vary along a straight line, reflecting an inverse relation without delay. Evidently, the increase in flow results in a decreased HbR, whereas a CBF decrease causes an elevation in HbR. These temporal relationships between ΔCBF and ΔHbR are consistent with two different physiological states: during the first period, $CMRO_2$ (and thus the HbR level) was elevated by the stimulation and the delayed blood flow caused a delayed reduction in HbR. The delayed and inverse relationship between ΔCBF and ΔHbR was caused by the decrease in $CMRO_2$, which slowly returned to equilibrium over this period. During the second period, when $CMRO_2$ was already at equilibrium, any change in ΔCBF was reflected directly as an inverse change in ΔHbR. Similarly, in Fig. 3*B*, we observed that blood volume changes (ΔCBV) lead the ΔCBF changes (ar-

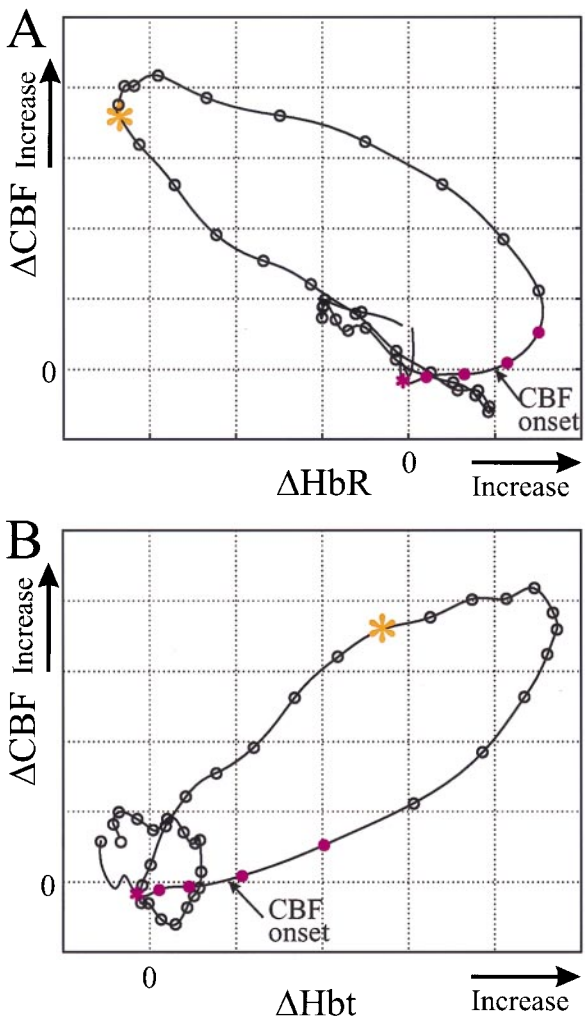

FIG. 3. Correlated dynamics of CBF to HbR and to Hbt for short stimulus. Phase plots show the dependence of CBF changes on HbR and Hbt after 2 sec of stimulation. Along the curves, intervals between the circles represent 0.5 sec, and the first four segments (five circles) are during stimulation. An asterisk marks the stimulus onset, and an arrow marks the onset of CBF, when an observable change in its rate of change is detected. (*A*) After stimulation onset (pink asterisk), HbR increases, whereas no observable change in CBF is seen for more than a second. As CBF starts to increase (arrow), the rate of change of HbR starts to decrease and becomes negative 1 sec later. At the last phase of the response (red asterisk), an inverse relation between the parameters is seen; an increase in CBF is accompanied by a decrease in HbR and *vice versa*. (*B*) An exponential dependence of CBF on Hbt is seen during the first 4.5 sec after stimulus onset. Throughout the response cycle, changes in Hbt lead changes in CBF by about 1–2 sec.

rows in Fig. 2*A* and an ellipsoid shape in Fig. 3*B*) throughout the response period.

The temporal relations between Hbt and CBF changes are not consistent with the hypothesis that blood flow changes induce blood volume changes, but rather the opposite! From these two phase plots one can hypothesize that the variations in Hbt induce blood flow changes throughout the response cycle. Sensory stimulation increases $CMRO_2$ (and thus HbR) and induces a perturbation in Hbt by local dilation of the vessels, which lasts for many seconds. The elevation of blood volume (and Hbt) induces a delayed blood flow change, which in turn induces a decrease in HbR. It is not possible to observe the changes in $CMRO_2$ selectively by monitoring HbR, because both $CMRO_2$ and flow induce changes in HbR. However, we may deduce the dynamics of $CMRO_2$ from the temporal relationship between ΔHbR and ΔCBF. While the $CMRO_2$ was slowly returning to baseline, HbR was delayed relative to CBF. At a later period (5–18 sec after stimulus termination; the beginning of this period is marked by the asterisk in Fig. 3*A*), any change in CBF was mirrored directly as an inverse change in HbR: an increase in flow causes a reduction in HbR whereas a decrease in flow causes an elevation in HbR. These results are consistent with constant $CMRO_2$ and functional recruitment of capillaries (see *Discussion*).

DISCUSSION

Correlation Between Imaging Spectroscopy and LDF. In the present study we used optical techniques to differentiate several manifestations of the vascular events associated with sensory activation of cortex. By using the spectrum of reflected light from activated cortex we were able to extract the alterations in blood oxygenation and total hemoglobin concentration. A simple linear model was used to estimate variations in HbR, HbO_2, and light-scattering components from the spectral changes. We were concerned that our model might not be sufficiently rigorous and that this might compromise the analytical results and their interpretation. In a previous report (13) we stated that the results were not sensitive to more complicated models of light scattering. The current study with simultaneous LDF measurements lends additional support to our previous conclusions, derived from imaging spectroscopy alone. In particular, we can consolidate our description of the sequence of vascular events following sensory activation. (*i*) As soon as blood flow, as measured by the LDF, increased, the HbO_2, as measured by imaging spectroscopy, also increased (Fig. 2). (*ii*) The rate of change in HbR started to decrease as soon as a blood flow increase was detected by the LDF measurement (Fig. 2*A Inset*). Thus, these two very independent measurements (e.g., imaging spectroscopy and LDF) provide mutually consistent results that strengthen the reliability of both methodologies.

Implications for fMRI. Functional activation of the human brain based on activity-dependent CBF responses can be imaged with PET or flow-sensitive MRI. However, optical imaging has shown that functional maps exclusively based on a this secondary vascular response may offer a lower spatial resolution than the initial HbR increase that is localized to the sites of elevated neuronal firing. The delayed HBO_2 increase occurred to an almost equal degree in both activated and nearby nonactivated cortical columns (compare figure 3 B and C in ref. 13). Because the delayed HBO_2 component, which originates from the blood flow increase, is poorly localized, its associated HbR decrease must also be poorly localized. We found that increasing the stimulus duration reduced the signal to noise in maps of functional cortical domains.

Most fMRI studies have been unable to detect the "initial dip" in blood oxygenation observed with optical imaging. However, a few recent studies indeed have confirmed that such an initial increase in HbR can be observed by using high-field-strength fMRI (14, 25). Consequently, the question of whether BOLD-fMRI can detect the very early increase in HbR currently is subject to controversy. The data presented here suggest that the early blood deoxygenation occurs concurrently with an increase in total hemoglobin concentration (Fig. 2*A*). It is possible that the increase in total hemoglobin concentration is accompanied by blood volume changes and by functional capillary recruitment, whose exact effects on the BOLD signals is not yet known. Thus, there is currently a disagreement between the dynamics of HbR, as measured by imaging spectroscopy and PO_2 as previously measured by an ion-selective microelectrode (26) on the one hand, and the BOLD signal, as measured by fMRI on the other. This question warrants extensive exploration.

Vascular Regulation at the Capillary Level. The present data and previous studies (8, 13) demonstrate that the metabolic consequence of functional activation (i.e., increased HbR because of increased O_2 demand) reaches the microvasculature less than 500 msec after stimulation onset. Interestingly, this increase in HbR cannot entirely be accounted for by deoxygenation of HbO_2, because we did not find the expected HbO_2 decrease. Rather, we observed that Hbt levels also increased at this early phase of the response, before the CBF change in the activated tissue. This apparently surprising fast increase in total hemoglobin concentration forced us to search for a suitable physiological mechanism that can explain these data. One possibility is that this early Hbt increase indeed reflects blood volume increase at the capillary bed, which currently is a controversial notion (27, 28). Regulation at the capillary level is also compatible with our ability to visualize individual functional columns whose size is often less than 200 μm, a size that would be too small to visualize if the regulation of blood volume were to occur in any of the other vascular compartments alone. Although capillaries per definition do not contain smooth muscle cells, they are surrounded by pericytes (29). This latter cell type is contractile and reacts to a number of stimuli implicated in cerebrovascular coupling (nitric oxide, drop in pH, ATP, adenosine) with dilatation. For this reason, pericytes have been suggested as an active element involved in capillary blood flow regulation (29).

"Functional Recruitment" of Capillaries. Functional recruitment (30) of capillaries is the transition of low-flow capillaries to high-flow capillaries (28). One might envision a very early phase of activation when local capillary corpuscular blood volume increases, but at a time when arterioles have not yet dilated and the blood flow has not yet increased. Although not very intuitive at first sight, this type of delayed relationship between blood volume and blood flow is possible if the outflow from the capillary compartment in the activated cortical columns is temporarily lower than the inflow to this capillary compartment. This type of scenario might arise if the capacitance of the capillaries were to increase and their resistance were to decrease following the electrical activity. In other words, because of the increased capacitance of this vascular compartment, where resistance is comparatively low, the capillary bed might act as "sink" for red blood cells, allowing the outflow from the compartment to drop, before the occurrence of upstream arteriolar dilatation that would cause an increased inflow. Subsequently, when the arteriolar segment has dilated, the increased inflow causes a flow increase in the entire capillary compartment, HbO_2 increases, and HbR decreases. Because in most cortical areas the arterioles do not feed selectively individual functional domains, this flow increase is less localized to the site of increased electrical activity.

The early functional capillary recruitment is consistent with our previous report (8). After loading the microcirculation with a fluorescent dextran, an increase in blood volume was detected in response to visual stimulation. The ability to obtain high-resolution functional maps upon selectively imaging these blood volume changes indicated that a significant portion of this change must have taken place in capillaries rather than another vascular compartment.

We thank Dr. Louis Sokoloff for his constructive comments. We also thank D. Ettner, N. Dekel, and C. Weijbergen for their technical support. This work was supported by grants from Ms. Margaret Enoch, the Minerva foundation, and the Wolfson Foundation to A.G.

1. Roy, C. & Sherrington, C. (1890) *J. Physiol.* **11,** 85–108.
2. Ketty, S. S. & Schmidt, C. F. (1945) *Am. J. Physiol.* **143,** 53–66.
3. Sokoloff, L., Reivich, M., Kennedy, C., Des Rosiers, M. H., Patlak, C. S., Pettigrew, K. D., Sakurada, O. & Shinohara, M. (1977) *J. Neurochem.* **28,** 897–916.
4. Chance, B., Cohen, P., Jobsis, F. & Schoener, B. (1962) *Science* **137,** 499–502.
5. Fox, P. & Raichle, M. (1985) *Ann. Neurol.* **17,** 303–305.
6. Raichle, M. (1994) *Sci. Am.* **270,** 58–64.
7. Grinvald, A., Lieke, E., Frostig, R. D., Gilbert, C. D. & Wiesel, T. N. (1986) *Nature (London)* **324,** 361–364.
8. Frostig, R. D., Lieke, E. E., Ts'o, D. Y. & Grinvald, A. (1990) *Proc. Natl. Acad. Sci. USA* **87,** 6082–6086.
9. Belliveau, J., Kennedy, D., McKinstry, R., Buchbinder, B., Weisskopf, R., *et al.* (1991) *Science* **254,** 716–719.
10. Ogawa, S., Tank, D., Menon, R., Ellerman, J., Kim, S., *et al.* (1992) *Proc. Natl. Acad. Sci. USA* **89,** 5951–5955.
11. Kwong, K., Belliveau, J., Chesler, D., Goldberg, I., Weisskoff, R., Poncelet, B., Kennedy, D., Hoppel, B., Cohen, M., Turner, R., Cheng, H., Brady, T. & Rosen, B. (1992) *Proc. Natl. Acad. Sci. USA* **89,** 5675–5679.
12. Turner, R., Jezzard, P., Wen, H., Kwong, K., Le Bihan, D., *et al.* (1993) *Magn. Reson. Med.* **277,** 279.
13. Malonek, D. & Grinvald, A. (1996) *Science* **272,** 551–554.
14. Menon, R. S., Ogawa, S., Hu, X., Strupp, J. P., Anderson, P. & Ugurbil, K. (1995) *Magn. Reson. Med.* **33,** 453–459.
15. Ts'o, D. Y., Frostig, R. D., Lieke, E. E. & Grinvald, A. (1990) *Science* **249,** 417–420.
16. Dirnagl, U., Kaplan, B., Jacewicz, M. & Pulsinelli, W. (1989) *J. Cereb. Blood Flow Metab.* **9,** 589–596.
17. Fabricius, M. & Lauritzen, M. (1996) *J. Cereb. Blood Flow Metab.* **16,** 156–161.
18. Haberl, R. L., Heizer, M. L., Marmarou, A. & Ellis, E. F. (1989) *Am. J. Physiol.* **256,** H1247–H1254.
19. Ratzlaff, E. H. & Grinvald, A. (1991) *J. Neurosci. Methods* **36,** 127–137.
20. LaManna, J. C., Sick, T. J., Pikarsky, S. M. & Rosenthal, S. M. (1987) *Am. J. Physiol.* **253,** C477–C483.
21. Stern, M. D. (1975) *Nature (London)* **254,** 56–58.
22. Bonner, R. & Nossal, R. (1981) *Appl. Opt.* **20,** 2097–2107.
23. Shepherd, A. P., Riedel, G. L., Kiel, J. W., Haumschild, D. J. & Maxwell, L. C. (1987) *Am. J. Physiol.* **252,** G832–G839.
24. Lindauer, U., Villringer, A. & Dirnagl, U. (1993) *Am. J. Physiol.* **264,** H1223–H1228.
25. Hu, X., Le, T. H. & Ugurbil, K. (1997) *Magn. Reson. Med.* **37,** 877–884.
26. Silver, I. (1978) in *Cerebral Vascular Smooth Muscle and Its Control*, eds. Elliott, K. & O'Connor, M. (Elsevier, New York), pp. 49–61.
27. Weiss, H. R. (1988) *Microvasc. Res.* **36,** 172–180.
28. Kuschinsky, W. & Paulson, O. B. (1992) *Cerebrovasc. Brain Metab. Rev.* **4,** 261–286.
29. Tilton, R. G. (1991) *J. Electron Microsc. Technol.* **19,** 327–344.
30. Villringer, A. & Dirnagl, U. (1995) *Cerebrovasc. Brain Metab. Rev.* **7,** 240–276.